ELSEVIER

Journal of Magnetism and Magnetic Materials 200 (1999) 741–754

Journal of magnetism and magnetic materials

www.elsevier.com/locate/jmmm

Polarized-neutron reflectometry

J.F. Ankner[a], G.P. Felcher[b,*]

[a]*Spallation Neutron Source, Oak Ridge National Laboratory, Oak Ridge, TN 37831, USA*
[b]*Material Science Division, Argonne National Laboratory, Building 223, Argonne, IL 60439, USA*

Received 25 February 1999; received in revised form 7 April 1999

Abstract

Polarized-neutron specular reflectometry (PNR) was developed in the 1980s as a means of measuring depth-resolved magnetization in flat films with characteristic thicknesses from 2 to 5000 Å. PNR has been widely used to study homogeneous and heterogeneous magnetic films, as well as superconductors. Starting from simple profiles, and gradually solving structures of greater complexity, PNR has been used to observe or clarify phenomena as diverse as the magnetism of very thin films, the penetration of fluxoids in superconductors, and the magnetic coupling across non-magnetic spacers. Although PNR is considered to be a probe of depth-dependent magnetic structure, laterally averaged in the plane of the film, the development of new scattering techniques promises to enable the characterization of lateral magnetic structures. Retaining the depth-sensitivity of specular reflectivity, off-specular reflectivity can resolve in-plane structures over nanometer to micron length scales. Presently limited by the neutron fluxes available, neutron reflectivity is expected to blossom in the next century, thanks to the increased brightness of the neutron beams, due not only to continuing improvements in neutron optics, but especially to the advent of second-generation spallation neutron sources.

PACS: 61.12.He; 78.70. – i

Keywords: Reflectometry; Polarized neutron; Magnetic thin films

1. Principles

The wave properties of the neutron make possible the optical study of matter by means of neutron beams [1,2]. As shown in Fig. 1, a beam of neutrons is reflected from a flat, laterally homogeneous object. The intensity of the reflected beam, recorded at different neutron wavelengths and angles of incidence, permits an evaluation of the chemical and magnetic depth profile. If the surface is corrugated, or if the material under the surface is not laterally homogeneous, the angle of the exiting neutrons may be different from that of the incoming beam, either in the reflection plane ($\alpha_i \neq \alpha_f$), or out of it ($\theta \neq 0$), depending on the geometry of the inhomogeneities.

The case of specular reflection is the simplest to treat. The momentum of the neutron, $|\boldsymbol{k}| = 2\pi/\lambda$ (where λ is the neutron wavelength), can be separated into two components, parallel and perpendicular to the surface. Only the perpendicular ($\hat{z}$)

* Corresponding author. Tel.: + 1-630-252-5516; fax: + 1-630-252-7777.
E-mail address: felcher@anl.gov (G.P. Felcher)

0304-8853/99/$ - see front matter
PII: S0304-8853(99)00392-3

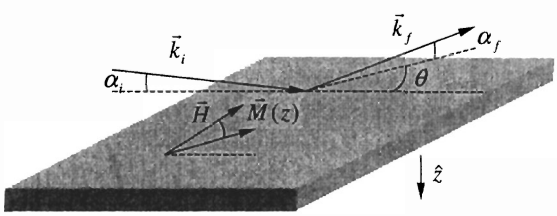

Fig. 1. Glancing angles of incidence (α_i) and exit (α_f) characterize experiments done in reflection geometry. For specular reflectivity, $\alpha_i = \alpha_f$ and $\theta = 0$. Neutrons polarized parallel to an externally applied field $\boldsymbol{H}$ are used to determine the depth profile of magnetization $\boldsymbol{M}(z)$ in the sample.

component is altered by the potential $U(z)$ describing the laterally homogeneous material. Thus, we can represent the neutron as a particle having kinetic energy $\hbar^2 k_z^2/2m$, hitting a potential wall of height $U(z)$. If its energy is too low, the neutron bounces back. A part of the potential, which is present in all matter, is simply related [3,4] to the scattering length b of the N constituent nuclei per unit volume: $U(z) = (\hbar^2/2m)N(z)b(z)$. For thermal and cold neutrons, the isotopic b is constant and conveniently tabulated for all nuclei (as well as for the natural isotopic composition of all elements). In free space (above the surface) $U(z) \approx 0$ and the neutron wave function is

$$u(z) = \exp(ik_z z) + r\exp(-ik_z z) \tag{1}$$

for a plane wave incident on the surface from above. The wave function inside the material is linked to the potential by the Schrödinger equation, whose solution gives the reflectance r. In a scattering experiment, the observed quantity is the reflectivity $R = |r|^2$. The wave vector transfer,

$$Q_z = k_{zf} - k_{zi} = \frac{4\pi \sin\alpha}{\lambda} \tag{2}$$

provides a convenient metric for characterizing the specular reflection process in which incident- and reflected-beam wave vectors ($\boldsymbol{k}_i$, $\boldsymbol{k}_f$) enter and exit the surface at the same glancing angle α [5]. Since momentum $\hbar Q_z$ is the quantum mechanical conjugate to position z, one can transform the depth profile of scattering material $b(z)$ into reflectivity $R(Q_z)$. The inverse process (from reflectivity to profile) is more complex, and will be discussed later. However, some simple rules give a flavor of the link between the two quantities.

In general, the reflectivity is unitary for most materials up to a value of $Q_c = \sqrt{16\pi Nb}$ of order 0.01 Å^{-1}. Beyond this limit, the reflectivity decreases rapidly with a mean asymptotic Q_z^{-4} dependence. For $Q_z \gg Q_c$, the reflectivity from a sequence of L layers is well described using the first Born approximation:

$$R \approx \frac{1}{Q_z^4}\left|4\pi \sum_{l=1}^{L} [(Nb)_l - (Nb)_{l-1}] \exp(iQ_z d_l)\right|^2, \tag{3}$$

where d_l is the distance of the lth layer's top interface below the surface.

Neutrons also interact with magnetic induction fields $\boldsymbol{B}$. In the presence of magnetic induction, the interaction potential becomes

$$U(z) = U_n(z) + U_m(z) = \frac{\hbar^2}{2m} N(z)b(z) + \boldsymbol{B}\cdot\hat{s}, \tag{4}$$

where $\hat{s}$ is the neutron spin operator [6]. Since the neutron is a spin-$\frac{1}{2}$ particle, there are two states of quantization with reference to an external magnetic field $\boldsymbol{H}$. In a measurement, the neutron may be polarized either parallel (+) or antiparallel (−) to $\boldsymbol{H}$. Suppose that the neutron is polarized in an applied field $\boldsymbol{H}_p$. Upon encountering an induction $\boldsymbol{B}_s$ with a different orientation (for instance inside a sample), the neutron changes its spin state. In classical terms, the neutron moment precesses about $\boldsymbol{B}_s$. The final state of the neutron may be analyzed in terms of the polarization with respect to a third field, $\boldsymbol{H}_a$. If, as is customarily done, $\boldsymbol{H}_a \| \boldsymbol{H}_p$, four reflectivities can be measured: R^{++}, R^{--}, R^{+-}, and R^{-+}.

The spin-dependent Schrödinger equation takes a very simple form when all of the magnetic induction in the neutron path is collinear. In this case, neutrons remain polarized in the original state ($R^{+-} = R^{-+} = 0$). Neutrons polarized parallel (+) [antiparallel (−)] to $\boldsymbol{H}_p$ see a potential $U^{\pm} = (\hbar^2/2m)Nb \pm \mu B$, where μ is the neutron magnetic moment. The magnetic medium is, in effect, birefringent. Since the strength of the magnetic scattering in ferromagnetic materials is comparable to that of the nuclear, an analysis of the

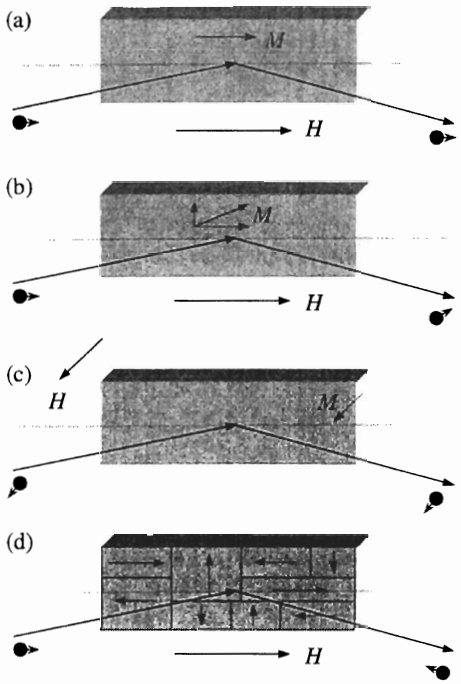

Fig. 2. The orientation and magnitude of the sample magnetization $\boldsymbol{M}(z)$ relative to the applied field $\boldsymbol{H}$ determines the relative proportions of spin-flip (SF) and non-spin-flip (NSF) scattering. (a) $\boldsymbol{M}(z)$ in the plane of the surface, parallel to $\boldsymbol{H}$ produces no SF scattering, but creates different spin-dependent refractive indices for neutrons polarized parallel and anti-parallel to $\boldsymbol{H}$. (b) $\boldsymbol{M}(z)$ canted at an arbitrary angle in the surface plane produces both SF and NSF intensity. (c) $\boldsymbol{M}(z)$ components normal to the surface have no effect on neutron specular intensity. (d) The presence of domains complicates interpretation of SF and NSF intensities. Off-specular methods offer a means of characterizing these domains.

reflectivities R^{++} and R^{--} makes possible a quantitative determination of $B(z)$. Components of $\boldsymbol{B}$ perpendicular to a sample surface are not directly detected by specular neutron reflectivity. By analogy with Eq. (3), neutrons are reflected by potential gradients across interfaces. Since $\nabla \cdot \boldsymbol{B} = 0$, perpendicular components of $\boldsymbol{B}$ are constant across a reflecting interface and therefore do not produce specularly reflected intensity [7].

Fig. 2 summarizes the phenomenology of magnetic reflection. A polarized neutron beam incident on a ferromagnetic layer aligned parallel to an external field exhibits no specular spin-flip scattering (Fig. 2a). However, the orientation of an in-plane ferromagnetic layer (Fig. 2b) can be determined by measuring the intensity of spin-flip relative to non-spin-flip scattering. When the magnetization is perpendicular to the surface (Fig. 2c), there is no difference in refractive index between neutrons polarized parallel and anti-parallel to $\boldsymbol{H}$. In the specularly reflected beam, such a sample is indistinguishable from one with no magnetization. The presence of domains and their size distribution strongly affects the specularly reflected intensity (Fig. 2d). The coherence length of the neutron beam on the surface is about 100 μm, larger than the lateral domain size in many samples. These small domains produce significant scattering off the specular beam, which also becomes depolarized. Currently, except in select instances, off-specular scattering cannot be quantitatively interpreted. Obtaining this in-plane structural information is one of the most significant motivations to develop off-specular scattering techniques and data analysis.

2. Instruments

A reflectometer is a simple instrument (Fig. 3) [8,9]. A neutron beam of wavelength λ strikes a sample surface at an angle α_i and is reflected from the surface at angle α_f. The instrument functions as a diffractometer with resolution sufficient to separate transmitted and reflected beams at values of Q_z near where the reflectivity becomes unitary. Specular reflectivity ($\alpha_i = \alpha_f$) is solely a function of the momentum transfer along the $\hat{z}$-direction, hence in practice a range of Q_z is spanned either by changing the wavelength, and keeping fixed the angle of incidence, or by changing the angle of incidence at fixed wavelength. Appropriate devices, such as polarizing mirrors and flat-coil spin flippers, polarize the incoming neutrons along an applied magnetic field or analyze the polarization of the reflected beam. Conventionally, the direction of initial polarization is fixed. The sample may change the polarization of the neutron and an analyzer chooses, among the reflected neutrons, those aligned with the polarizer. Reversal of the neutron spin is obtained by energizing flippers placed before and

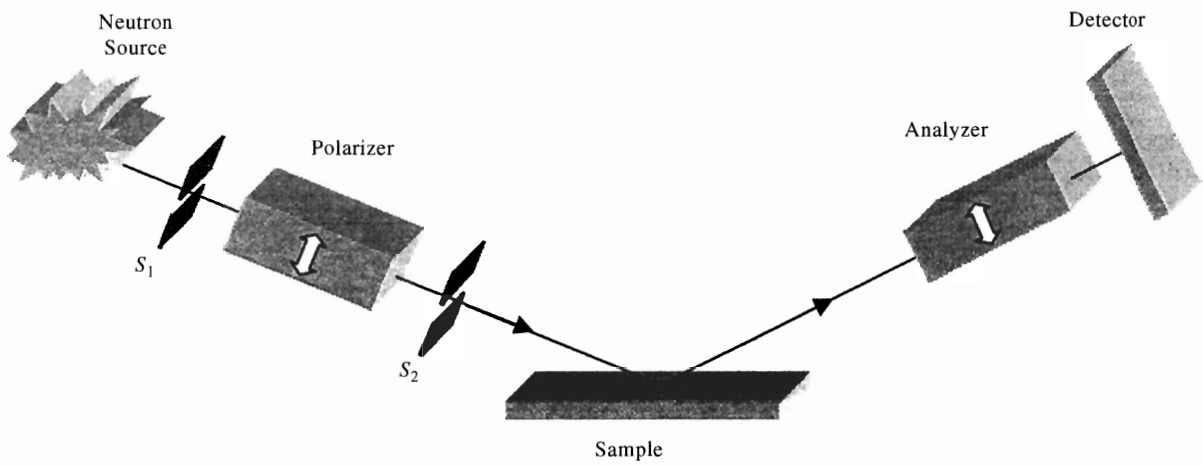

Fig. 3. Neutron reflectometers at both fixed-wavelength and broadband sources consist of the same general components: a reactor or spallation neutron source, two slits s_1 and s_2 to define the incident-beam collimation, incident-beam polarizing and spin-flipping elements, a flat sample on a positioning table, exit-beam polarization analysis, and a position-sensitive or single detector.

after the sample. The reflectivities are then characterized by the sign of the neutron polarization before and after reflection with respect to the reference field: R^{++}, R^{--}, R^{+-}, and R^{-+}.

As an example, Fig. 4 plots the spin-dependent reflectivity of a multilayer of Fe/Cr in which the magnetization of successive Fe layers is non-collinear [10]. The presence of $R^{\pm\mp}$ specular intensity is a signature of magnetic order perpendicular to the applied field. In some circumstances, the interpretation of this scattering is straightforward. For instance, Fig. 4b exhibits a Bragg reflection at $Q_z = 0.045$ Å^{-1}, entirely of magnetic origin. The peak arises from a series of magnetic layers, alternately magnetized in opposite directions (AF). The non-spin-flip ($R^{\pm\pm}$) and spin-flip ($R^{\pm\mp}$) reflectivities are, respectively, proportional to $M_{\parallel}$ and $M_{\perp}$, the projections of the staggered magnetization parallel and perpendicular to the neutron polarization axis. After making a similar analysis of the ferromagnetic peak (at $Q_z = 0.09$ Å^{-1}), one can determine the angle between the two sublattice magnetizations. For other values of Q_z, the relationship between spin-dependent reflectivities and spin structure is not transparent and details of the non-collinear structure are obtained by model fitting.

3. Data modeling

As outlined above, calculating the specular reflectivity of polarized neutrons from a sequence of homogeneous refracting slabs entails a straightforward application of the solution of the one-dimensional Schrödinger equation. By selecting fine enough depth increments, one can model arbitrarily complex $b(z)$ and $\boldsymbol{B}(z)$. After collecting reflectivity in the four spin states R^{++}, R^{--}, R^{+-}, and R^{-+}, and accounting for such effects as background scattering and polarization efficiency, one begins with a model of the sample based on prior knowledge of its growth conditions [11,12]. The nuclear and magnetic structure of the film can then be determined by adjusting the parameters of this model to fit the data.

As an example of this process, consider the specular reflectivity of a sputtered (59 Å Fe/49 Å Si)$_{13}$/ glass multilayer shown in Fig. 5. These data [13] were taken in saturation, with Fe layer moments aligned parallel to the applied field, and therefore exhibit no spin-flip scattering. Fig. 5a shows the data from the (+ +) spin state and Fig. 5b the (− −). The gray lines result from a model in which the iron layers exhibit uniform magnetization. Note in particular how poorly this model

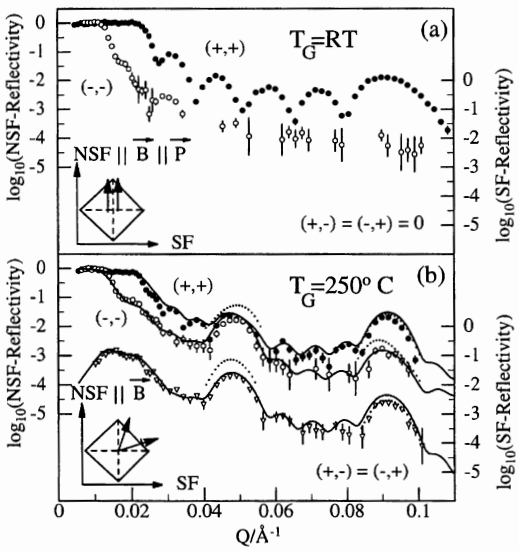

Fig. 4. Spin-polarized neutron specular reflectivity data measured in remanence ($H = 30$ Oe) from two superlattices featuring the same layer thicknesses, 52 Å Fe/17 Å Cr, prepared at two different growth temperatures T_G. (a) The sample grown at room temperature produces no spin-flip (SF) scattering and its non-spin-flip (NSF) intensity is consistent with a model in which successive Fe layers are aligned with the applied field. (b) The sample prepared at $T_G = 250$°C exhibits strong SF scattering which, when modeled with the NSF intensity, reveals that successive Fe layers align symmetrically with respect to the sample anisotropy axes (inset) at an unusual angle (from Ref. [10]).

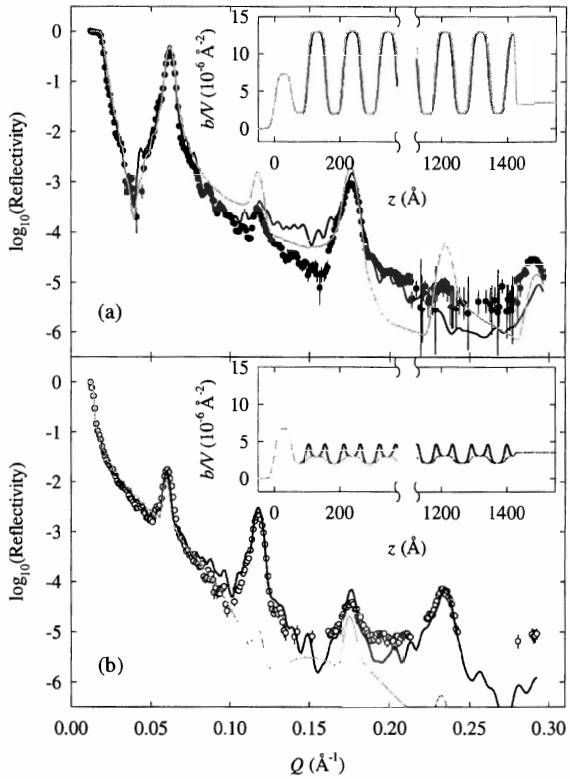

Fig. 5. Spin-polarized reflectivity data from a [59 Å Fe/49 Å $Si]_{13}$/glass multilayer. The Fe layers are aligned with the 300-Oe applied field, so there is no spin-flip scattering. (a) The data taken with neutron polarization parallel to $\boldsymbol{H}$ for a simple model with uniform Fe layer magnetization (gray) and one including layer thickness disorder and 6.2-Å thick interfacial magnetic dead layers. (b) The data with the neutron polarization antiparallel to $\boldsymbol{H}$ are very sensitive to the presence of the magnetic dead layer, particularly the second and fourth superlattice harmonics (from Ref. [13]).

fits the (− −) data in the vicinity of the second ($Q_z = 0.115$ Å^{-1}) and fourth ($Q_z = 0.23$ Å^{-1}) superlattice peaks. However, by postulating 6-Å-thick magnetically dead (or disordered, recall Fig. 2d) layers in the Fe at the Si interface, one achieves a much better fit to the data (black lines). As can be seen from the scattering density profiles in the insets, the presence of the dead layers has little effect on the (+ +) superlattice intensities, but profoundly changes the (− −), effectively halving the multilayer periodicity and thereby enhancing the intensities of even-order superlattice reflections. A relatively subtle interfacial effect produces a distinct signature in the polarized-neutron reflectivity data.

As with other scattering techniques, measurements of the reflected intensity $R = |r|^2$ lose the phase information required for a unique determination of sample structure. Consequently, very different scattering density profiles may produce specular reflectivities that are statistically similar. There have been a number of recent advances in direct inversion of reflectivity data that, in principle, retain the phase of r, by means of the addition of two or three reference layers [14–17]. Even if the sample to be examined is non-magnetic, it may be convenient to add a reference layer that is ferromagnetic. In such a system, the reference layer has different reflectance when analyzed with neutrons of opposite polarization state. The practical applicability of

this approach, to eliminate ambiguities stemming from the non-uniqueness of fitting procedures, is presently the object of intensive research.

A brief review will be given in the following sections of the scientific themes that have been pursued up to now. There will also be a presentation of those for which the quest has not yet been successful, but which show promise of being solved in the near future.

4. Superconducting films

Historically, the first published polarized-neutron specular reflectometry (PNR) experiment measured the London penetration depth in a superconductor. The penetration depth characterizes completely the diamagnetism of a film for applied magnetic fields below H_{c1}, the field at which magnetic flux is expelled from the bulk. Values of the penetration depth determined at different laboratories have converged satisfactorily. This is not only true of conventional superconductors, like niobium [18,19], but also of the high-T_c superconductor $YBa_2Cu_3O_{7-x}$, where measurements point to a penetration depth of the order of 1000 Å (see Fig. 6) [20,21]. In this respect, PNR now rivals other techniques, such as muon spin resonance. At the same time, analysis of the data allows a verification of the detailed depth dependence of the magnetic field penetration into the surface, up to now assumed to have (with the exception of pure type-I superconductors) exponential form.

Above H_{c1}, an inhomogeneous state is created in type-II superconductors, with the magnetic field penetrating along lines of fluxoids. Arrays of fluxoids have been observed with surface-sensitive techniques when the magnetic field is applied perpendicular to the surface. With the field parallel to the surface, the fluxoids may remain entirely within the material. Under these circumstances, a penetrating probe such as neutron reflection should be the tool of choice.

The nature of magnetic configurations above H_{c1} is still under discussion. From transport measurements, it appears that the configuration of fluxoids is not universal, but depends strongly on

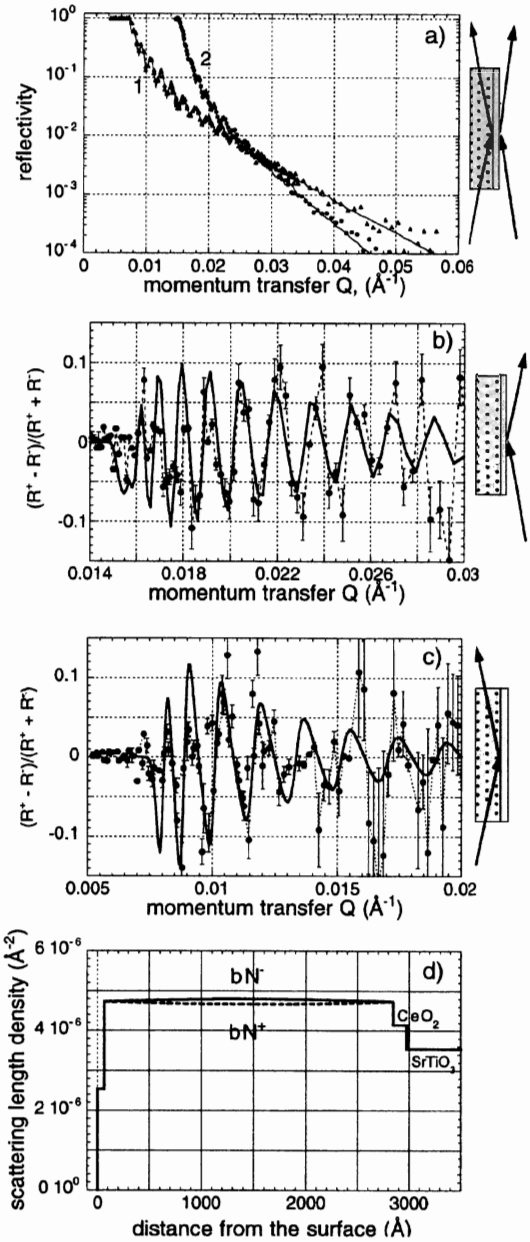

Fig. 6. The London penetration depth ($\lambda_L = 1350 \pm 150$ Å) of a $YBa_2Cu_3O_7$ film is determined to high precision by consistent modeling of non-spin-flip specular intensity taken with the beam incident both from vacuum and from within the $SrTiO_3$ substrate. (a) The reflectivity measured incident from the substrate (1) and from vacuum (2). (b) Spin asymmetry $[(R^{++} - R^{--})/(R^{++} + R^{--})]$ plotted with beam incident from vacuum and (c) from substrate. (d) Neutron scattering density plotted as a function of depth for the two spin states, showing sensitivity to small refractive index differences (from Ref. [21]).

the anisotropy of the coherence lengths, the thickness of the superconducting layers, and the density of pinning centers. The only anisotropy present in a single film of niobium is shape anisotropy. Material anisotropy can be introduced by layering thin films of superconductor with metallic spacers (epitaxially grown high-T_c materials represent an extreme case). In all cases, pinning centers may give rise to a disordered distribution of fluxoids not aligned with the field but straggling through the film. The magnetic response is then well described by the Bean model [22]. In the absence of pinning centers, fluxoids should order into a lattice. When the anisotropy is extreme, the fluxoid currents are located principally within the superconducting layers, minimizing the tunneling through the non-superconducting layers (Josephson vortices). For less anisotropic media, a different organization of fluxoids has been suggested [23]: above H_{c1}, a single line of flux forms at the center of the film to minimize the repulsion from either surface.

In practice, geometrical conditions severely restrict the range of observable fluxoid lattice spacings, and the intensity of the diffraction line is expected to be very weak. Up to now, the presence of a fluxoid lattice has been inferred only from the spin dependence of the specular reflectivity. The effect of fluxoids on the specular reflectivities depends on their concentration as a function of z. If pinned at random, their effect would only be seen close to the total reflection wave vector ($Q_z \approx Q_c$). However, a line of fluxoids located at the center of a superconducting film of thickness d gives rise to a maximal spin dependence of the reflectivity at $Q_z \approx 2\pi/(d/2)$. This solution has been found to be consistent with reflectivity measurements on $YBa_2Cu_3O_7$ [24,25]. On the other hand, an array of Josephson fluxoids in a multilayer is expected to exhibit a maximal spin dependence of the reflectivity at the Bragg reflections of the multilayer. A response of this kind has been observed in Nb/Si multilayers [26].

5. Magnetization in single films

In films less than a few nanometers thick, magnetic materials are significantly altered from the bulk in magnitude, direction, and type of magnetic order. These new properties result from a complex set of circumstances, such as incomplete quenching of the orbital moments, tension or compression of the lattice on the substrate, and transfer of electrons between magnetic film and substrate. Polarized neutron reflection has been used to determine the absolute value of the magnetic moment per atom (notably in Fe and Co) in very thin films (see Fig. 7) [27–31]. The results are in good agreement with those theoretically predicted, as well as those obtained by alternative techniques [32,33].

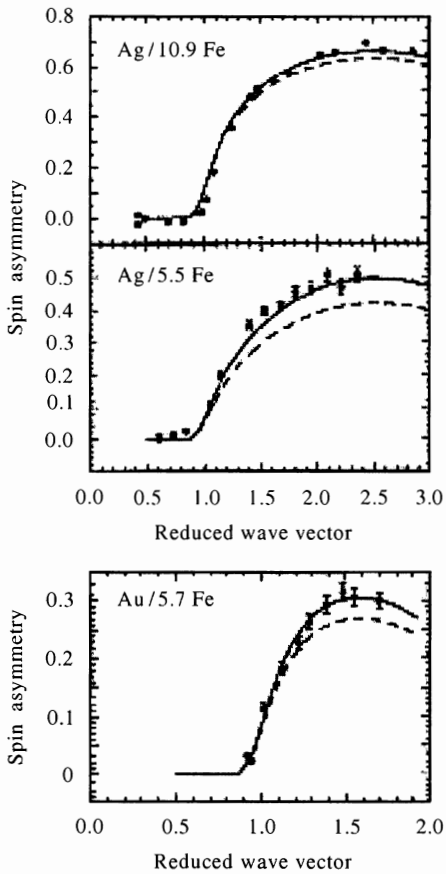

Fig. 7. Enhanced magnetic moment is observed in thin buried Fe layers. The dashed lines plot the neutron spin asymmetry $[(R^{++} - R^{--})/(R^{++} + R^{--})]$ expected for Fe exhibiting the bulk moment. Fitted curves (solid lines) are consistent with enhanced moments that become more pronounced for thinner films (from Ref. [28]).

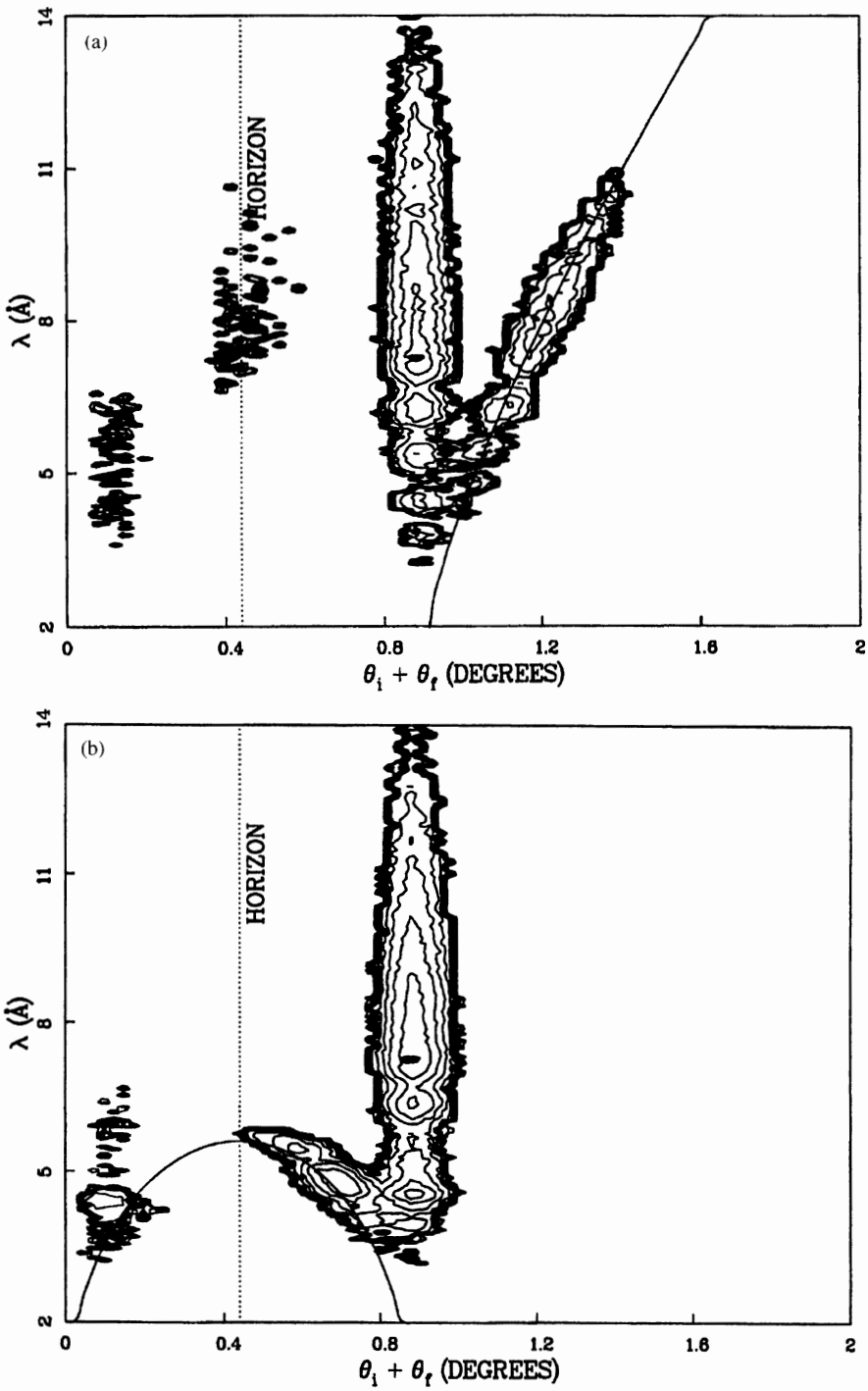

Fig. 8. Reflectivity from a 1000-Å thick film of Co on Si. A magnetic field $H = 13$ kOe was applied perpendicular to the surface. This field was insufficient to overcome shape anisotropy. The in-plane component of the magnetization therefore induces neutron spin-flip scattering in the reflected beam. The change in reflected exit angle ($\alpha \equiv \theta$ in the figure) for the spin-flipped neutrons depends on the square of wavelength times applied field normal to the surface $\lambda^2 H^2$. (a) Shows R^{++} as vertical and R^{+-} as wavelength-dispersed contours; (b) vertical R^{--} with wavelength-dispersed R^{-+} contours (from Ref. [34]).

Off-specular spin-flip magnetic scattering has been observed in large external magnetic fields. The prototype experiments were carried out on a film of ferromagnetic cobalt. The natural magnetization of this film lies in the plane of the surface. A magnetic field $\boldsymbol{H}$, applied perpendicular to the surface, was insufficient to overcome this shape anisotropy. However, some of the reflected neutrons flipped their spin, thereby exchanging potential energy (by the amount of the Zeeman splitting) with kinetic energy. From the laws of conservation of energy and momentum for the spin-flipped neutrons, one can derive the condition $\alpha_f^2 = \alpha_i^2 \pm 1.47 \times 10^{-7}\lambda^2 H^2$ (α_i and α_f are the incident and reflected angles in radians, H is expressed in kOe, and λ in Å) [34–36]. Spin-flipped neutrons are reflected at angles significantly different from the angle of incidence (Fig. 8) even in fields of a few kOe. The Zeeman splitting physically separates neutrons of opposite spin.

In addition to measuring layer-averaged magnetization as a function of depth via specular reflectivity, one can also study surface magnetic structure on atomic length scales by means of grazing-angle diffraction. If incident and exit angles (α_i and α_f in Fig. 1) are kept below the critical angle for total reflection, then the penetration depth of the neutron evanescent wave below the sample surface is limited to 50–100 Å for most materials [37]. Intensity measured by scanning θ through a surface-plane Bragg reflection then arises solely from atoms confined to this thin surface layer. Fig. 9a shows the intensity of the (1 1 0) surface Bragg peak of an Fe(1 0 0) film as a function of α_i and α_f; Fig. 9b the results of a model calculation [38]. The neutrons are initially unpolarized, yet the diffracted intensities I^{++}, I^{--}, I^{+-}, and I^{-+} appear at different spots. Within the ferromagnetic material, neutrons of opposite spin effectively have a different wavelength (as a result of refraction). The novel result of this experiment is the presence of non-negligible I^{+-} and I^{-+}. A layer of iron fully magnetized parallel to the surface should exhibit no spin-flip intensity. Its presence is the signature of magnetic moments directed perpendicular to the surface, possibly due to scattering from a disordered native oxide layer. Sensitivity to surface-normal magnetic components and to atomic order

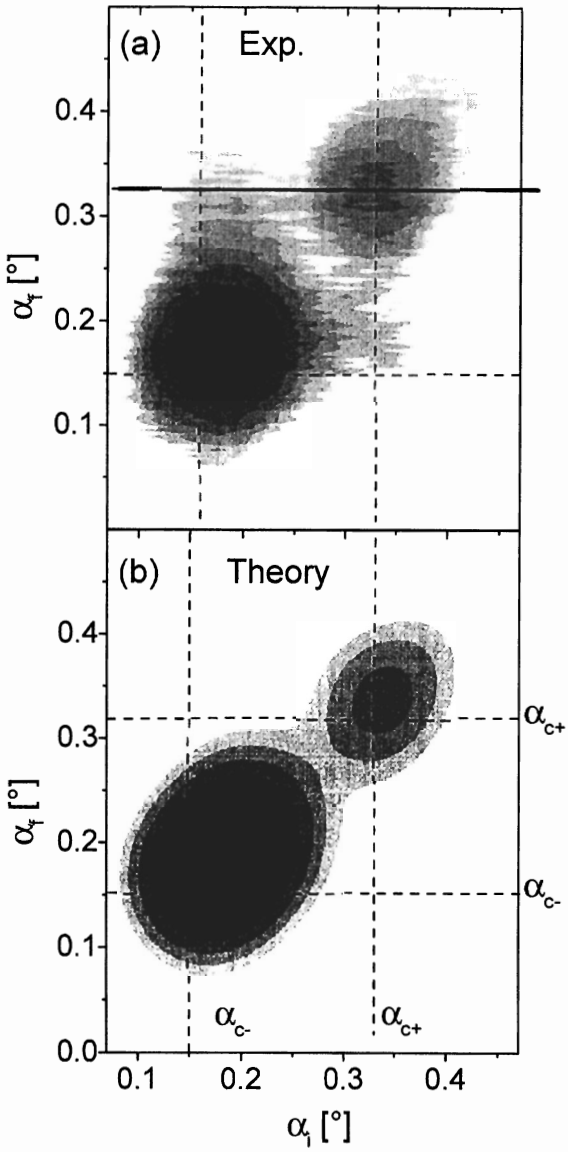

Fig. 9. Grazing-angle diffraction measurement of the (1 1 0) surface Bragg reflection from an Fe(1 0 0) film. (a) Intensity contours measured as a function of incident (α_i) and exit (α_f) reflection angles basically confirm a simple model based on uniformly magnetized Fe, according to which I^{--} has a maximum when $\alpha_i = \alpha_f = \alpha_{c-} \approx 0.19°$, while I^{++} has a maximum at $\alpha_i = \alpha_f = \alpha_{c+} \approx 0.32°$. The presence of auxiliary maxima near $(\alpha_i, \alpha_f) = (\alpha_{c\pm}, \alpha_{c\mp})$ reveals the presence of spin-flip scattering, caused by perpendicular moment components in the oxide layer (from Ref. [38]).

(inaccessible to specular reflectivity measurements), as well as depth resolution, are compelling advantages of grazing-angle diffraction which may outweigh the difficulties of the technique.

6. Coupling between magnetic layers

Exchange anisotropy, a phenomenon discovered almost 50 years ago, remains unexplained today. The requirements for observing exchange anisotropy are satisfied when a ferromagnetic (F) and an anti-ferromagnetic material (AF) are in contact, and F orders magnetically at a temperature higher than that of AF. Upon cooling the F/AF couple in a magnetic field to below the Néel temperature of AF, the sample's magnetization loop remains permanently biased in the direction of the cooling field. All models hitherto proposed explain this magnetic behavior in terms of a configuration of spins at the F/AF interface in which AF spins do not fully switch when the F layer's magnetization reverses [39]. Unfortunately, none of these models fully explains the effect.

In the simplest model, the AF layer is composed of atomic planes with uncompensated spins. Interfacial AF atoms align with the bias field and do not flip when the magnetization is reversed. To study the magnetic depth profile in the proximity of a buried interface, PNR is, in principle, an excellent probe, provided that the F/AF pairs are prepared as thin films on flat surfaces. Yet, in experiments on Co/CoO and Permalloy/FeMn pairs [40,41], the measured reflectivities for the two neutron spin states were identical, even when reflectivities calculated on the basis of the models above were significantly different. In contrast, measurements [42] on an Fe_3O_4/NiO multilayer revealed magnetic differences in the two saturated states of the magnetic hysteresis loop, due possibly to interfacial domain wall formation in the ferrimagnetic Fe_3O_4 layers.

In an alternative model [43], the AF atomic planes parallel to the interface are compensated, and the AF moments align at 90° (spin flop) with respect to F. Some features of this model have been tested in a recent experiment [44] on Co/CoO. The AF CoO layer was composed of domains whose population changed with the direction of the magnetization in F. AF domains with a sublattice magnetization perpendicular to that of the F layer were statistically slightly favored. More definite 90° coupling has been found in Fe_3O_4/CoO superlattices [45] between ferrimagnetic Fe_3O_4 and antiferromagnetic CoO layers.

In perhaps the most intriguing model proposed [39], AF consists of domains of very limited lateral extent (of the order of a few tens of Angstroms). With a finite number of spins in a domain at the interface, it becomes statistically possible to induce exchange bias as a residual effect. If this were the case, the AF layers would not contribute to specular reflectivity but would give rise instead to a diffuse distribution of intensity either in the forward direction or in wide-angle diffraction at grazing incidence. Experiments of this kind require more powerful neutron sources.

The interaction between two ferromagnetic layers interleaved with a metallic spacer that is either non-magnetic or weakly AF, depends strongly on the nature and thickness of the spacer. PNR studies have been conducted on Fe/Cr/Fe [47] and Co/Cu/Co [46] sandwiches. If the two magnetic layers are unequal in either thickness, chemistry, or because one is anchored to an antiferromagnet, the system may behave as a spin-valve. PNR has been used to measure the magnetization of each layer of such sandwiches [48,49], confirming the results inferred by magnetization measurements.

7. Magnetic multilayers

First for a few selected pairs, then for a host of combinations of Fe, Co, Ni interleaved by most of the 3, 4, and 5d transition metals, it was found that the coupling between successive ferromagnetic layers oscillates from ferromagnetic (F) to antiferromagnetic (AF) as the thickness of the non-magnetic spacers varies. Magnetic fields ranging from several to a few thousand Oersted saturate the magnetization of AF-coupled multilayers, with a corresponding large change of magnetoresistance. The magnetic structure predicted for the AF state is of type $+ - + -$, a simple doubling of the chemical periodicity d. This structure has been confirmed

directly by PNR. In this case, the basic PNR experiment consists of measuring the intensity of Bragg reflections at values of $2\sin\theta/\lambda$ equal to $1/d$ and $1/2d$: the first gives information on the ferromagnetic contribution of the average bilayer, the second on the AF contribution. A number of authors have observed this magnetic configuration in different systems, studied the pattern of antiferromagnetic domains, their evolution with the application of a magnetic field, and the correlation with magnetoresistance [50–55]. However, PNR measurements have been applied to perform a considerably more sophisticated analysis in certain of these systems.

In the course of studying Fe/Cr superlattices, it was sought to correlate the magnetization of Fe with the spin density wave (SDW) in Cr. The SDW gives rise to magnetic satellites around the Cr(0 0 1) diffraction line [56,57]. From the relative intensities of these diffraction lines, it has been found that the period of the SDW and even its phase vary systematically with Cr layer thickness.

In general, to determine the details of the magnetic profile of the repeat unit of a superlattice, a large Q_z region needs to be explored. Bragg reflections appear, for a typical bilayer thickness of a few tens of Angstroms, at intervals $\Delta Q_z \sim 0.1$–0.2 Å^{-1}. An even more detailed description can be obtained for epitaxially grown superlattices, by measuring the intensities of the diffraction lines due to the mean atomic spacings ($Q_z \sim 2$ Å^{-1}) and their superlattice satellites. For Gd/Y superlattices [58], Bragg diffraction was used to infer the existence of magnetic dead layers at the interface.

Analysis of the polarization state of reflected neutrons has been used to determine depth- and direction-dependent magnetization. By this means, it was confirmed that in coupled multilayers with weak interlayer interactions, magnetic configurations forming 90° or other angles exist, as justified if biquadratic terms in the magnetic exchange become important [10,56,59–62].

The study of off-specular magnetic scattering has attracted increasing attention in recent years. Inhomogeneities in the plane of the film give rise to scattering which, in general, appears at reflected angles $\alpha_f \neq \alpha_i$ and $\theta \neq 0$ (recall Fig. 1). If an FM or an AF multilayer consists of in-plane domains, its magnetism is no longer uniform in the plane of the film, and the finite size of the domains gives rise to scattering around the direction of the reflected beam. This has been repeatedly observed (Fig. 10) [63–66]. From the width of this diffuse scattering domain sizes have been deduced. A rigorous theoretical framework for interpreting the data would make these measurements far more useful.

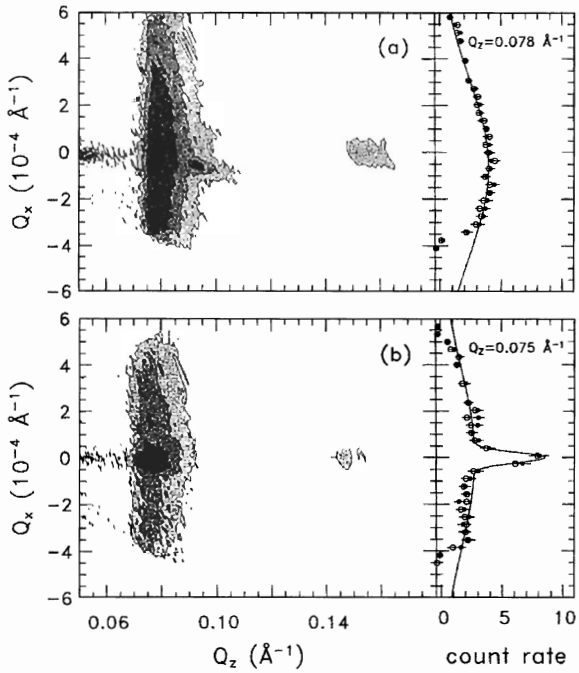

Fig. 10. Antiferromagnetic diffuse scattering measured in a [30 Å Fe/10 Å Cr] superlattice. (a) Prior to annealing, the film exhibits strong diffuse scattering along a ridge of Q_x centered on $Q_z = 0.078$ Å$^{-1} \approx 2\pi/(2 \times 40$ Å). In contrast, the peak at $Q_z = 0.16$ Å$^{-1} \approx 2\pi/40$ Å, indicative of the chemical modulation, is purely specular. The prominent half-order ridge of intensity is caused by 0.7 μm in-plane domains antiferromagnetically coupled to underlying layers. (b) After annealing at 350°C, a specular peak is visible, revealing a partial coalescence of small domains into domains larger than the coherence length of the neutrons (from Ref. [65]).

Less studied, but of growing interest, are multilayers involving rare earths interleaved with transition elements [67–70]. In multilayers of rare-earth/Fe or rare-earth/Co, both components are

magnetically ordered. For example, in Gd/Fe multilayers, the magnetization vectors of the Gd and Fe layers are oppositely directed, but in general are not compensated. A weak magnetic field is sufficient to orient the resulting ferrimagnetic moment, but not to disrupt the magnetic configuration. Increasing the field is predicted to cause a phase transition from the ferrimagnetic to a twisted configuration, sensitive to the atoms in the outermost interfacial layers [71]. If the excess interfacial magnetization is due to Fe, the magnetization of the Fe-terminated face should be more readily directed toward the applied magnetic field than that of the Gd layer that terminates the opposite face. PNR measurements are indeed consistent with this overall model and eventually should be able to provide a detailed picture of the orientation of the magnetization throughout the multilayer. In a single Fe/Gd bilayer, it has been found that the soft Gd–Gd exchange interaction causes a twist of the magnetization within the Gd layer [72,73].

Recently, La/Fe multilayers were constructed that exhibit a fragile helical magnetic structure, stable in time, but permanently destroyed after application of a field of 100 Oe. This effect turned out to result from imprinting during film deposition, rather than by interlayer coupling [74]. Each layer was 30 Å thick, and during deposition the sample was rotated in an external field of 3 Oe, strong enough to magnetize the Fe layer being deposited but not sufficient to perturb the magnetization of the Fe layers already grown. As revealed by PNR, adjacent Fe layers formed a helical structure with a chirality and periodicity determined by the rotational direction and speed of the substrate and the rate of deposition.

Hydrogenation changes reversibly the band structure and metallic character of the components of a multilayer in a selective way, and by an amount controllable with the hydrogen pressure. In Nb/Fe and V/Fe superlattices, it has been shown [75,76] that hydrogen enters solely in the Nb and V lattices. Magnetically, the effect of hydrogenation is to switch reversibly between the AF- and FM-coupled states (Fig. 11). In rare earth/transition element multilayers, the formation of rare-earth hydrides greatly reduces the structural mismatch between the crystal lattices. Here the reversibility is between the rare earth RH_2 and RH_3 states.

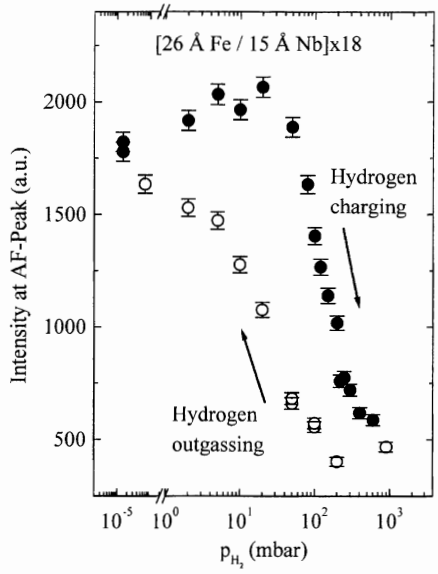

Fig. 11. The change in magnetic coupling induced by charging an Fe/Nb superlattice with hydrogen. AF coupling strength passes through a peak and then abruptly declines with increasing hydrogen pressure (from Ref. [75]).

8. The future

The exercise of predicting future development is challenging and, when viewed in retrospect, amusing. However, it is fair to say that the next decade will see important technical developments. PNR is sorely limited by the brightness of current neutron sources. A new generation of high-flux pulsed neutron sources being designed and built in the United States, and planned for Europe and Japan, will increase the available neutron flux by an order of magnitude. At the same time, efforts are underway to utilize these fluxes more efficiently. In the 1990s, the development of supermirrors has allowed better piping of neutrons to the sample position, but gains hitherto have been due to flat mirrors. The next several years should see developments of focusing optics based on curved mirrors or (a field yet largely untouched) magnetic lenses. Finally, ongoing

developments in spin-polarized ^{3}He devices [77] for the polarization analysis of polychromatic, divergent beams should revolutionize off-specular magnetic reflectivity research and other areas of neutron scattering.

Concurrently with the development of hardware, a robust effort is underway to develop more powerful and transparent methods of data analysis. Much progress has been made recently on direct inversion methods for determining the magnetic profile from reflectivity without a priori assumptions. In addition, the full utilization of three-dimensional neutron spin analysis, with analogies to be drawn from nuclear magnetic resonance, has yet to be explored. Finally, for off-specular scattering, the problem of data modeling is significantly more complicated than for specular scattering. Yet, the potential of off-specular scattering geometries to address important problems in magnetism has only recently and tentatively been exploited. By measuring intensity away from the specular beam, one samples wave vector components Q_x in the plane of the surface, instead of averaging over them, as does specular reflectivity. Sensitivity to these in-plane structures is especially important in magnetic materials, where domain formation is such a ubiquitous phenomenon (recall Fig. 2d). The ability of neutrons to see below the surface and to discriminate as a function of depth confers particular advantages relative to specifically surface-sensitive techniques.

We have seen in the preceding paragraphs how specular reflectivity of polarized neutrons has been applied to a broad range of magnetic problems. Some of these problems have been solved successfully. For others, a more satisfactory solution requires greater resolution and/or sensitivity. An order of magnitude improvement in dynamic range over current instruments would make routine the resolution of atom-scale structures. One could then measure the full spectrum of sample lengths from thousands of Angstroms to inter-atomic spacings in a single specular measurement. Higher fluxes will also allow new ventures, such as the study of the kinetics and dynamics of the magnetization process. Finally, future new applications and science will no doubt be stimulated by the construction and fabrication of novel magnetic systems, such as arrays of magnetic dots.

Acknowledgements

This work was supported by US-DOE DE-AC05-960R22464 and US-DOE, BES-MS contract 31-109-ENG-38. The authors would like to thank J.A.C. Bland, W. Donner, F. Klose, V. Lauter-Pasyuk, and A. Schreyer for providing figures used in the text.

References

[1] A.G. Klein, S.A. Werner, Rep. Prog. Phys. 46 (1983) 259.
[2] M. Born, E. Wolf, Principles of Optics, 6th edition, Pergamon, Oxford, 1980.
[3] E. Fermi, W. Zinn, Phys. Rev. 70 (1946) 103.
[4] E. Fermi, I. Marshall, Phys. Rev. 71 (1947) 666.
[5] J. Lekner, Theory of Reflection, Nijhoff/Kluwer, Amsterdam, 1987.
[6] D.J. Hughes, Pile Neutron Research, Addison-Wesley, Cambridge, 1953.
[7] S.J. Blundell, J.A.C. Bland, Phys. Rev. B 46 (1992) 3391.
[8] G.P. Felcher, R.O. Hilleke, R.K. Crawford, J. Haumann, R. Kleb, G. Ostrowski, Rev. Sci. Instr. 58 (1987) 609.
[9] C.F. Majkrzak, Physica B 173 (1991) 75.
[10] A. Schreyer, J.F. Ankner, M. Schäfer, H. Zabel, C.F. Majkrzak, P. Grunberg, Physica B 221 (1996) 366.
[11] J.F. Ankner, C.F. Majkrzak, in: C.F. Majkrzak, J.L. Wood, Neutron Optical Devices and Applications, SPIE Conference Proceedings, Vol. 1738, SPIE, Bellingham, Washington, 1992, pp. 260–269.
[12] X.L. Zhou, S.H. Chen, Phys. Rep. 257 (1995) 223.
[13] J.F. Ankner, C.F. Majkrzak, H. Homma, J. Appl. Phys. 73 (1993) 6436.
[14] C.F. Majkrzak, N.F. Berk, Phys. Rev. B 52 (1995) 10827.
[15] V.O. deHaan, A.A. van Well, S. Adenwalla, G.P. Felcher, Phys. Rev. B 52 (1995) 10831.
[16] J. Kasper, H. Leeb, R. Lipperheide, Phys. Rev. Lett. 80 (1998) 2614.
[17] C.F. Majkrzak, N.F. Berk, Phys. Rev. B 58 (1998) 15416.
[18] M. Maaza, L.P. Chernenko, D. Korneev, B. Pardo, C. Sella, F. Bridou, Phys. Lett. A 218 (1996) 312.
[19] H. Zhang, J.W. Lynn, C.F. Majkrzak, S.K. Satija, J.H. Kang, X.D. Wu, Phys. Rev. B 52 (1995) 10395.
[20] J.M. Reynolds, V. Nunez, A.T. Boothroyd, T. Fretolft, D.G. Bucknall, J. Penfold, Physica B 248 (1998) 163.
[21] V. Lauter-Pasyuk, H.J. Lauter, V.L. Aksenov, E.I. Kornilov, A.V. Petrenko, P. Leiderer, Physica B 241–243 (1997) 1095.
[22] Jan Evetts (Ed.), Encyclopedia of Magnetic and Superconducting Materials, Pergamon Press, Oxford, 1992, p. 95.
[23] J. Guimpel, L. Civale, F. de la Cruz, N.J. Koeman, D.G. de Groot, R. Griessen, B.I. Ivlev, Phys. Rev. Lett. 71 (1993) 2319.
[24] V. Lauter-Pasyuk, H.J. Lauter, V.L. Aksenov, E.I. Kornilov, A.V. Petrenko, P. Leiderer, Physica B 248 (1998) 166.
[25] S.-W. Han, J.F. Ankner, H. Kaiser, P.F. Miceli, E. Paraoanu, L.H. Greene, Phys. Rev. B, in press.

[26] S.M. Yusuf, E.E. Fullerton, R.M. Osgood, G.P. Felcher, J. Appl. Phys. 83 (1998) 6801.
[27] H. Fritzsche, T. Nawrath, H. Maletta, H. Lauter, Physica B 241 (1997) 707.
[28] J.A.C. Bland, J. Lee, S. Hope, G. Lauhoff, J. Penfold, D. Bucknall, J. Magn. Magn. Mater. 165 (1997) 46.
[29] J.A.C. Bland, C. Daboo, G.A. Gehring, B. Kaplan, A.J.R. Ives, R.J. Hicken, A.D. Johnson, J. Phys.: Condens. Matter 7 (1995) 6467.
[30] J.A.C. Bland, C. Daboo, B. Heinrich, Z. Celinski, R.D. Bateson, Phys. Rev. B 51 (1995) 258.
[31] J. Lee, G. Lauhoff, C. Fermon, S. Hope, J.A.C. Bland, J.P. Schille, G. Vanderlaan, C. Chappert, P Beauvillain, J. Phys.: Condens. Matter 9 (1997) L137.
[32] Z. Celinski, K.B. Urquhart, B. Heinrich, J. Magn. Magn. Mater. 166 (1997) 6.
[33] S. Hope, J. Lee, P. Rosdenbusch, G. Lauhoff, J.A.C. Bland, A. Ercole, D. Bucknall, J. Penfold, H.J. Lauter, V. Lauter, R. Cubitt, Phys. Rev. B 55 (1997) 11422.
[34] G.P. Felcher, S. Adenwalla, V.O. deHaan, A.A. van Well, Nature 377 (1995) 409.
[35] D.K. Korneev, V.I. Bodnarchuk, V.K. Ignatovich, J. Phys. Soc. Jpn. Suppl. A 65 (1996) 37.
[36] H. Fredrikze, Th. Rekveldt, A. van Well, Y. Nikitenko, V. Syromyatnikov, Physica B 248 (1998) 157.
[37] H. Dosch, B.W. Batterman, D.C. Wack, Phys. Rev. Lett. 56 (1986) 1144.
[38] R. Günther, W. Donner, B. Toperverg, H. Dosch, Phys. Rev. Lett. 81 (1998) 116.
[39] A.P. Malozemoff, Phys. Rev. B 35 (1987) 3679.
[40] S.S.P. Parkin, V.R. Deline, R.O. Hilleke, G.P. Felcher, Phys. Rev. B 42 (1990) 10583.
[41] G.P. Felcher, Y.Y. Huang, M. Carey, A. Berkowitz, J. Magn. Magn. Mater. 121 (1993) 105.
[42] A.R. Ball, A.J.G. Leenaers, P.J. van der Zaag, K.A. Shaw, B. Singer, D.M. Lind, H. Fredrikze, M.Th. Rekveldt, Appl. Phys. Lett. 69 (1996) 1489.
[43] N.C. Koon, Phys. Rev. Lett. 78 (1997) 4865.
[44] J.A. Borchers, Y. Ijiri, S.-H. Lee, C.F. Majkrzak, G.P. Felcher, K. Takano, R.H. Kodama, A.E. Berkowitz, J. Appl. Phys. 83 (1998) 7219.
[45] Y. Ijiri, J.A. Borchers, R.W. Erwin, S.-H. Lee, P.J. van der Zaag, R.M. Wolf, Phys. Rev. Lett. 80 (1998) 608.
[46] J.A.C. Bland, H.T. Leung, S.J. Blundell, V.S. Speriosu, S. Metin, B.A. Gurney, J. Penfold, J. Appl. Phys. 79 (1996) 6295.
[47] A.J.R. Ives, J.A.C. Bland, T. Thomson, P.C. Riedi, M.J. Walker, J. Xu, D. Greig, J. Magn. Magn. Mater. 154 (1996) 301.
[48] J.A.C. Bland, C. Daboo, M. Patel, T. Fujimoto, J. Penfold, Phys. Rev. B 57 (1998) 10272.
[49] A. Van der Graaf, A.R. Ball, J.C.S. Kools, J. Magn. Magn. Mater. 165 (1997) 479.
[50] A. Van der Graaf, M. Valkier, J. Kohlhepp, F.J.A. den Broeder, J. Magn. Magn. Mater. 165 (1997) 157.
[51] J.A. Borchers, P.M. Gehring, R.W. Erwin, C.F. Majkrzak, J.F. Ankner, T.L. Hylton, K.R. Coffey, M.A. Parker, J.K. Howard, J. Appl. Phys. 79 (1996) 4762.
[52] M. Mao, S.H. Nguyen, B.D. Gaulin, Z. Tun, X. Bian, Z. Altounian, J.O. Stromolsen, J. Appl. Phys. 79 (1996) 4769.
[53] N. Hosoito, K. Mibu, T. Ono, T. Emoto, T. Shinjo, J. Magn. Magn. Mater. 156 (1996) 325.
[54] J.A. Borchers, P.M. Gehring, R.W. Erwin, J.F. Ankner, C.F. Majkrzak, T.L. Hylton, K.R. Coffey, M.A. Parker, J.K. Howard, Phys. Rev. B 54 (1996) 9870.
[55] D.E. Joyce, S.I. Campbell, P.R.T. Pugh, P.J. Gruny, Physica B 248 (1998) 152.
[56] E.E. Fullerton, S. Adenwalla, G.P. Felcher, K.T. Riggs, C.H. Sowers, S.D. Bader, J.L. Robertson, Physica B 221 (1996) 370.
[57] P. Bödeker, A. Schreyer, P. Sonntag, C. Sutter, G. Grübel, R. Günther, H. Zabel, Physica B 248 (1998) 114.
[58] C.F. Majkrzak, J. Kwo, M. Hong, Y. Yafet, D. Gibbs, C.L. Chien, J. Bohr, Adv. Phys. 40 (1991) 99.
[59] J. Kohlhepp, M. Valkier, A. Van der Graaf, F.J.A. den Broeder, Phys. Rev. B 55 (1997) R696.
[60] S. Adenwalla, G.P. Felcher, E.E. Fullerton, S.D. Bader, Phys. Rev. B 53 (1996) 2474.
[61] A. Schreyer, J.F. Ankner, T. Zeidler, H. Zabel, M. Schäfer, J.A. Wolf, P. Grunberg, C.F. Majkrzak, Phys. Rev. B 52 (1995) 16066.
[62] A. Schreyer, J.F. Ankner, T. Zeidler, H. Zabel, C.F. Majkrzak, M Schäfer, P. Grünberg, Europhys. Lett. 32 (1995) 595.
[63] G.P. Felcher, Physica B 192 (1993) 137.
[64] Y. Endoh, M. Takeda, A. Kamijo, J. Mizuki, N. Hosoito, T. Shinjo, Mater. Sci. Eng. B 31 (1995) 57.
[65] W. Hahn, M. Loewenhaupt, G.P. Felcher, Y.Y. Huang, S.S.P. Parkin, J. Appl. Phys. 75 (1994) 3564.
[66] V. Syromyatnikov, B. Toperverg, V. Deriglazov, A. Schebetov, T. Ebel, R. Kampmann, R. Wagner, Physica B 234 (1997) 575.
[67] Y. Li, C. Polaczyk, J. Kapoor, F. Klose, F. Mezei, Riegel, Physica B 234 (1997) 492.
[68] M.C. Luche, A. Baudry, P. Boyer, J.L. Rouviere, C. Fermon, C. Miramond, J. Magn. Magn. Mater. 150 (1995) 175.
[69] J. Tappert, F. Klose, C. Rehm, W.S. Kim, R.A. Brand, H. Maletta, W. Keune, J. Magn. Magn. Mater. 158 (1996) 317.
[70] W. Hahn, M. Loewenhaupt, Y.Y. Huang, G.P. Felcher, S.S.P. Parkin, Phys. Rev. B 52 (1995) 16041.
[71] J.G. LePage, R.E. Camley, Phys. Rev. Lett. 65 (1990) 1152.
[72] F.K. McGrath, N. Ryzhanova, C. Lacroix, D. Givord, C. Fermon, C. Miramond, G. Saux, S. Young, A. Vedyayev, Phys. Rev. B 54 (1996) 6088.
[73] Y. Li, C. Polaczyk, F. Mezei, D. Riegel, Physica B 234 (1997) 489.
[74] G.P. Felcher, W. Lohstroh, H. Fritzsche, M. Münzenberg, H. Maletta, W. Felsch, Appl. Phys. Lett. 72 (1998) 2894.
[75] F. Klose, C. Rehm, D. Nagengast, H. Maletta, A. Weidinger, Phys. Rev. Lett. 78 (1997) 1150.
[76] B. Hjörvarsson, J.A. Dura, P. Isberg, T. Watanabe, T.J. Udovic, G. Andersson, C.F. Majkrzak, Phys. Rev. Lett. 79 (1997) 904.
[77] K.P. Coulter et al., Nucl. Instr. Meth. A 288 (1990) 463.